COMMUNICATIONS PHYSICS

ARTICLE

https://doi.org/10.1038/s42005-020-00442-x OPEN

Parametric dependence of hot electron relaxation timescales on electron-electron and electron-phonon interaction strengths

Richard B. Wilson[1,2]✉ & Sinisa Coh[1,2]✉

Understanding how photoexcited electron dynamics depend on electron-electron (e-e) and electron-phonon (e-p) interaction strengths is important for many fields, e.g. ultrafast magnetism, photocatalysis, plasmonics, and others. Here, we report simple expressions that capture the interplay of e-e and e-p interactions on electron distribution relaxation times. We observe a dependence of the dynamics on e-e and e-p interaction strengths that is universal to most metals and is also counterintuitive. While only e-p interactions reduce the total energy stored by excited electrons, the time for energy to leave the electronic subsystem also depends on e-e interaction strengths because e-e interactions increase the number of electrons emitting phonons. The effect of e-e interactions on energy-relaxation is largest in metals with strong e-p interactions. Finally, the time high energy electron states remain occupied depends only on the strength of e-e interactions, even if e-p scattering rates are much greater than e-e scattering rates.

---

[1] Materials Science and Engineering, University of California, Riverside, CA 92521, USA. [2] Mechanical Engineering, University of California, Riverside, CA 92521, USA. ✉email: rwilson@ucr.edu; sinisacoh@gmail.com

Absorption of light by a metal generates a nonthermal distribution of electrons and holes[1–3]. In the femtoseconds to picoseconds following absorption, a complex cascade process emerges from individual electron–electron (e–e) and electron–phonon (e–p) scattering events[4–6]. This cascade process drives the system into a new equilibrium state.

We characterize the emergent nonequilibrium electron cascade process with two time-scales, τ_H and τ_E. Time τ_H measures how long the metal contains highly excited electrons with energy comparable to that of the incoming photons, $h\nu$. Somewhat arbitrarily, we define τ_H as the time for the number of highly excited electrons with energy greater than or equal to $h\nu/2$ to drop by a factor of $1/e$, see Fig. 1. Another emergent time scale shown in Fig. 1 is τ_E. Time τ_E is the time required for the total energy stored by all nonequilibrium electrons to drop by a factor of $1/e$.

Time-scales τ_E and τ_H are critical, and distinct, figures of merit for a variety of scientific and engineering endeavors, such as photocatalysis, ultrafast magnetism, and others. Ultrafast magnetic phenomena are commonly driven by τ_E because they depend on how quickly spatial gradients in internal energy are relaxed[7–13]. On time-scales shorter than τ_E, nonequilibrium electrons transport energy at rates that are 1–2 orders of magnitude faster than is possible after electrons and phonons thermalize[7,11,14–16]. On the other hand, several recent studies suggest photocatalytic performance of plasmonic metal nanoparticles is governed by τ_H[17–20]. High energy electrons are hypothesized to drive chemical reactions[17–20]. However, this hypothesis remains controversial because it is difficult to differentiate the effect of temperature rises from the effect of high energy nonequilibrium electrons[21,22].

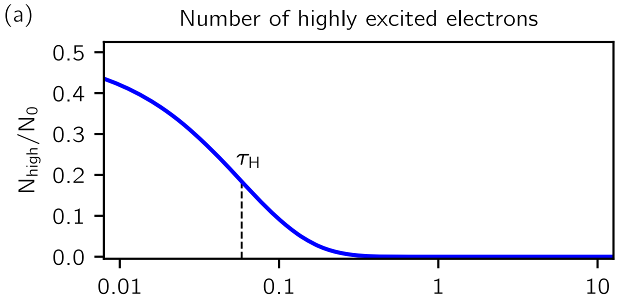

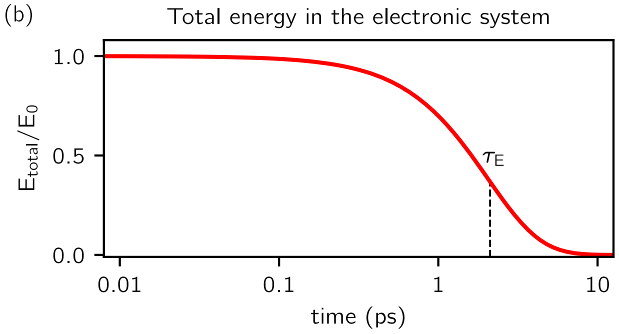

Fig. 1 Definitions of distribution relaxation time-scales τ_H and τ_E. We define time-scales τ_H and τ_E to characterize two distinct effects of quasiparticle interactions on nonequilibrium electron dynamics. τ_H measures how quickly electron–electron and electron–phonon interactions redistribute energy from high to low energy electronic states. τ_E measures how quickly electron–electron and electron–phonon interactions cause energy transfer from the electronic subsystem to the lattice. **a** After excitation with energy $h\nu$, the occupation states where $|\varepsilon| \geq h\nu/2$ decays with time τ_H. Here, we show τ_H for Au. **b** The energy absorbed by the electrons remains in the electronic subsystem for time τ_E. In Au, τ_E is 35 times greater than τ_H.

The fundamental importance of electron dynamics has motivated extensive theoretical[4,9,15,17,18,23–28] and experimental[2,5,6,29–38] study of relaxation times like τ_E and τ_H. These prior studies provide descriptions of how nonequilibrium electron distributions in specific materials like Au, Al, and Cu evolve as a function of time[5,23,24,29–31,39]. Early work by Tas and Maris[5] and Groeneveld et al.[29] found the e–e scattering increases the rate of energy transfer to the lattice by increasing the number of excitations. Time-resolved two-photon photoemission studies have found e–e interactions cause high energy electrons to decay on time-scales of tens of femtoseconds after photoexcitation[32]. Mueller and Rethfeld provided a detailed analysis of how various aspects of the collision integrals and rate-equations effect nonequilibrium electron dynamics in Au, Al, and Ni[24]. Other studies have integrated first-principles calculations of band-structure[40], photon absorption[17,18,41], and e–p interactions[17,18] into models for nonequilibrium electron dynamics to improve agreement with experiment. Recent work by the plasmonics community has focused on understanding how hot electrons effect photocatalytic efficiencies in plasmonic systems[3,21,22,42–46].

Surprisingly, no systematic study of how τ_E and τ_H depends on e–e vs. e–p interactions exists. As a result, significant confusion persists regarding the best method for estimating τ_E and τ_H from material properties such as quasiparticle lifetimes. Estimates in the literature for the energy relaxation time τ_E of various metals[26] almost always underestimate the importance of e–e interactions[5,23,24,29,31,39]. By far the most common method for estimating τ_E of a metal is the two-temperature model[26,28,47]. The two-temperature model neglects nonthermal effects, and therefore neglects the important role of e–e interactions. Alternatively, the relaxation time of high energy electrons τ_H is often incorrectly estimated from a simplified Boltzmann rate equation with a Matthiessen's-like rule[44,48–50], resulting in $\tau_H^{-1} \approx \tau_{ee}^{-1} + \tau_{ep}^{-1}$. Here τ_{ep} is the electron–phonon quasiparticle scattering time, and τ_{ee} is the electron-electron quasi-particle scattering time. This treatment leads to the incorrect conclusion that, since e–p scattering rates are stronger than e–e scattering rates, τ_H depends on the strength of e–p interactions. In other-words, the Matthiessen's rule estimate for the relaxation times of a nonequilibrium electron distribution will dramatically overestimate the importance of e–p interactions.

Here, we present the calculations of the dynamics of photo-excited electrons to quantify how τ_E and τ_H depend on electron–electron (e–e) and electron–phonon (e–p) interaction strengths. In contrast to the two-temperature model prediction of $\tau_E = \gamma_{ep}^{-1}$, we find nonthermal effects result in $\tau_E \approx 2.5\gamma_{ep}^{-0.75}\beta_{ee}^{-0.25}$. Here γ_{ep} and β_{ee} are measures of e–p and e–e interaction strength. γ_{ep} is the two-temperature model prediction for the energy relaxation rate[28]. β_{ee} is the electron–electron relaxation rate for an electron/hole 0.5 eV above/below the Fermi level. We find that the energy relaxation time τ_E remains sensitive to e–e scattering unless τ_E is at least two orders of magnitude larger than τ_H. Alternatively, we find the dependence of τ_H on e–e versus e–p interactions is quite different than for τ_E. We find that in most cases, due to differences in the nature of e–e vs. e–p interactions, the time-scale for high energy electrons to relax, τ_H, will depend primarily on e–e interactions. For photoexcitation with $h\nu \geq 2$ eV, τ_H depends only on e–e quasiparticle lifetimes. This is true even if e–p quasiparticle lifetimes, τ_{ep}, are hundreds of times shorter than e–e quasiparticle lifetimes, τ_{ee}. In order for τ_H to be sensitive to e–p scattering rates, $h\nu$ needs to be in the near-infrared, e.g., ~1 eV, and γ_{ep}/β_{ee} must be larger than 0.5. γ_{ep}/β_{ee} is larger than 0.5 for metals with light elements, e.g., Al, Cu, Li, and Mo. Our findings for τ_H agree with prior studies on nonequilibrium electron dynamics that found the lifetime of photoexcited electrons depends only on e–e quasiparticle lifetimes[1,23,32].

Results

Equation of motion for nonequilibrium electron dynamics. To accurately capture the interplaying effects of electron–electron and electron–phonon scattering on the dynamics, we solve the equation of motion for the electron distribution function in a simple metal,

$$\frac{\mathrm{d}f(\varepsilon,t)}{\mathrm{d}t} = \Gamma_\mathrm{ee}(f(\varepsilon,t)) + \Gamma_\mathrm{ep}(f(\varepsilon,t)). \tag{1}$$

Here ε is electron's energy relative the Fermi-level, Γ_ee is the e–e collision integral[27], and Γ_ep is the e–p collision integral[28]. Equation (1) accounts for both increases and decreases in $f(\varepsilon, t)$ due to scattering events. As a result, the dynamics predicted by Eq. (1) are different from the simple exponential functions arrived at by applying the relaxation-time-approximation. Since we are interested in the time-evolution of the nonequilibrium electrons, we linearize Eq. (1) by defining the nonequilibrium distribution as $\phi(\varepsilon,t) = f(\varepsilon,t) - f_0(\varepsilon,T_\mathrm{p})$. Here f_0 is the thermal Fermi–Dirac distribution and T_p is the temperature of the lattice. Our use of the phrase nonequilibrium electrons, or hot electrons, refers to the electrons and holes described by $\phi(\varepsilon, t)$.

The two-temperature model is a special limit of Eq. (1). The two-temperature model assumes $f(\varepsilon, t)$ is described by Fermi–Dirac statistics with an electron temperature T_e distinct from T_p. For this special limit[28], Eq. (1) reduces to a simple heat-equation,

$$C_\mathrm{e}\frac{\partial T_\mathrm{e}}{\partial t} = g_\mathrm{ep}\left[T_\mathrm{p} - T_\mathrm{e}\right]. \tag{2}$$

Here C_e is the electron heat-capacities and $g_\mathrm{ep} = (\pi\hbar k_\mathrm{B}D_\mathrm{F})\lambda\langle\omega^2\rangle$. D_F is the density of states at the Fermi level, and $\lambda\langle\omega^2\rangle$ is the 2nd frequency moment of the e–p spectral function[28]. $\lambda\langle\omega^2\rangle$ is a measure of the strength of e–p interactions at the Fermi-level (see "Methods" section and Supplementary Notes 1, 2). The dynamics of T_p are typically described with a 2nd heat-equation for the phonon subsystem (not shown here). The two-temperature model predicts an energy relaxation rate of $\gamma_\mathrm{ep} = g_\mathrm{ep}(C_\mathrm{p}^{-1} + C_\mathrm{e}^{-1})$[51]. At room temperature, where $C_\mathrm{p} >> C_\mathrm{e}$, this simplifies to $\gamma_\mathrm{ep} \approx g_\mathrm{ep}/C_\mathrm{e}$. The two-temperature model energy relaxation rate depends only on the strength of e–p interactions in the metal, $\gamma_\mathrm{ep} \approx 3\hbar\lambda\langle\omega^2\rangle/(\pi k_\mathrm{B}T)$[28].

Dynamics depend on quasiparticle interaction strengths. To quantify the parametric dependence of τ_E and τ_H on the strength of both e–e and e–p interactions, we need descriptors of the e–e and e–p interaction strengths. Somewhat arbitrarily, we choose γ_ep and β_ee as descriptors of the e–e and e–p interaction strength. γ_ep^{-1} is the τ_E predicted by the two-temperature model[28], while β_ee^{-1} is the e–e relaxation time for 0.5 eV excitations, $\beta_\mathrm{ee} = \tau_\mathrm{ee}^{-1}(\varepsilon = 0.5\,\mathrm{eV})$. There are a variety of other physical properties that would serve equally well as descriptors. We discuss descriptor choice in more detail in "Methods" section. In Table 1, we report literature values for γ_ep and β_ee for various metals.

We summarize the dynamics predicted by Eq. (1) in Fig. 2. Figure 2a shows the total number of nonequilibrium electrons vs. time for different ratios of e–p to e–e interaction strength $\gamma_\mathrm{ep}/\beta_\mathrm{ee}$. Figure 2b shows how the energy distribution of nonequilibrium electrons evolves with time. For realistic values of e–e interaction and e–p interaction strengths, e.g., $\gamma_\mathrm{ep}/\beta_\mathrm{ee} \approx 0.25$, e–e scattering increases the number of nonequilibrium electrons by about a factor of 5 on a τ_E time-scale. Alternatively, for infintely strong e-e interactions, $\gamma_\mathrm{ee}/\beta_\mathrm{ee} \to 0$, the energy stored in the initial nonthermal distribution instantly redistributes into a thermal distribution and Eq. (2) governs the dynamics. A thermalized electron distribution has ~16× as many exictations as are initially photo-excited. In contrast to the the energy distribution shown in Fig. 2b, approximately 90% of excitations in a thermal distribution are within ~100 meV of the Fermi-level. The difference between these two cases of realistic vs. infintiely strong e–e interactions is sometimes discussed in terms of a maximum equivalent effect temprature $\Delta T_\mathrm{e}^\mathrm{me}$. $\Delta T_\mathrm{e}^\mathrm{me}$ is defined as the temperature increase of a thermalized electron gas for the same injected energy[31,40,45].

In Supplementary Figs. 1–3, we show dynamics for Pt, Au, and Al. Specifically, we show the time-evolution of the occupation vs. energy, $\phi(\varepsilon)$, and energy-distribution vs. energy, $\varepsilon\phi(\varepsilon)$. The metals Pt, Au, and Al were chosen to illustrate dynamics for metals with small, typical, and large values of $\gamma_\mathrm{ep}/\beta_\mathrm{ee}$ in Table 1, respectively. In Supplementary Movies 1 and 2, we show the time-evolution of $\phi(\varepsilon)$ for Au as a function of time passing on a linear and logarithmic rate, respectively.

Our results for $\phi(\varepsilon, t)$ yield dynamics like those reported in many prior studies that solved Eq. (1) without using the relaxation-time-approximation[5,6,18,24,29,31,39]. Prior studies of nonequilibrium dynamics that solve the collision integrals in Eq. (1) have focused on specific material systems, e.g., Al, Au, Cu, and Ag[18,24,29,31,39]. New to our study is explicit consideration of how dynamics evolve across a wide range of e–e and e–p scattering strengths. Our predictions for the dynamics of $\phi(\varepsilon)$ differ significantly from prior studies that incorrectly approximate Eq. (1) with a relaxation-time approximation[1,2,35,44,50]. Models that use relaxation-time type approximations will predict τ_H values that are too short, because they assume e–p interactions effect τ_H. Furthermore, many relaxation-time models, like the modified two temperature model[52], assume the time-scale for a nonequilibrium electron distribution to thermalize is approximately equal to τ_H. We find the time-scale for thermalization is comparable to τ_E.

Dependence of τ_H and τ_E on quasiparticle interaction strengths. From $\phi(\varepsilon, t)$ predicted by Eq. (1), we determine relaxation times τ_H and τ_E as a function of e–p and e–e interaction strengths. Figure 3 shows how τ_H (time for high energy electrons to decay into lower energy electrons) and τ_E (time for energy of the nonequilibrium electrons to be transferred to the lattice) depend on $\gamma_\mathrm{ep}/\beta_\mathrm{ee}$. Figure 3 is the primary result of our study. We observe that τ_H and τ_E possess a universal dependence on the ratio of e–p to e–e scattering strengths. We find that in nearly all metals, $\gamma_\mathrm{ep}/\beta_\mathrm{ee}$ is such that τ_H depends only on e–e, while τ_E is determined by both e–e and e–p. To illustrate this universal dependence, we report τ_E normalized by γ_ep^{-1}, and τ_H normalized by β_ee^{-1}. The slope of $\tau_\mathrm{E}\gamma_\mathrm{ep}$ vs. $\gamma_\mathrm{ep}/\beta_\mathrm{ee}$ is determined by the sensitivity of τ_E to e–e interactions. A slope of zero indicates that energy exchange between electrons and phonons is not affected by the strength of e–e interactions. Similarly, the slope of $\tau_\mathrm{H}\beta_\mathrm{ee}$ vs. $\gamma_\mathrm{ep}/\beta_\mathrm{ee}$ is determined by the sensitivity of τ_H to e–p interactions. A slope of zero indicates the time for high energy electrons to decay into lower energy electrons is determined only by e–e interactions.

Discussion

We now discuss the origins for the dependence of τ_E and τ_H on β_ee and γ_ep. For most metals, high energy electrons decay with $\tau_\mathrm{H} \approx C\beta_\mathrm{ee}^{-1}$, where $C \approx 0.8\,\mathrm{eV}^2/(h\nu)^2$ with our model

Table 1 Literature values for the electron-electron and electron-phonon interaction strengths, β_{ee} and γ_{ep}, of various metals.

Metal	$\lambda\langle\omega^2\rangle$ (meV$^2/\hbar^2$)	Θ_D (K)	τ_{ep} (fs)	γ_{ep}^{-1} (fs)	β_{ee}^{-1} (fs)	τ_E (fs)	τ_H(fs)
Li	160	340	12	110	55	230	11
Na	13	158	29	1400	34	1600	7
K	3.4	91	37	5200	20	5500	4
Rb	1.8	56	27	9900	17	1.0×10^4	3
Cs	0.85	38	25	2.1×10^4	14	2.1×10^4	3
Ta	190	240	4.6	93	17	150	
Mo	240	450	13	74	57	170	
Fe	280	470	12	63	7.5	92	
Rh	350	480	10	51	12	89	
Ni	230	450	13	77	14	120	
Pd	130	270	8.6	140	8	170	
Pt	140	240	6.1	100	8	160	
Cu	57	340	31	310	160	650	30
Ag	23	230	34	790	300	1500	60
Au	15	170	27	1200	300	2100	60
Al	270	430	10	67	40	150	8
Gd	90	200	7	200	28	290	
Tb	90	200	7	200	18	270	

We use the electron-electron and electron interaction strengths to calculate τ_H, the time-scale high energy electronic states remain occupied for, and τ_E, the time-scale for energy transfer between the electronic subsystem and lattice. The values for the second frequency moment of the Eliashberg function $\lambda\langle\omega^2\rangle$ and Debye temperature Θ_D are from Allen[59], Kittel[61], and Papaconstantopoulos et al.[62]. To highlight the large discrepancy between electron–phonon quasiparticle scattering time τ_{ep} and time-scales τ_H and τ_E, we show $\tau_{ep} \approx \hbar/(2\pi\lambda k_B T)$ for each metal. However, we emphasize that τ_{ep} is not an input into our model. The values for β_{ee}^{-1} for the alkali metals are predictions from Fermi-liquid theory for a homogenous electron gas[32]. The values for β_{ee}^{-1} of other metals are from two photon photoemission data[32], except for Pt. We assume β_{ee}^{-1} for Pt is equal to β_{ee}^{-1} for Pd.

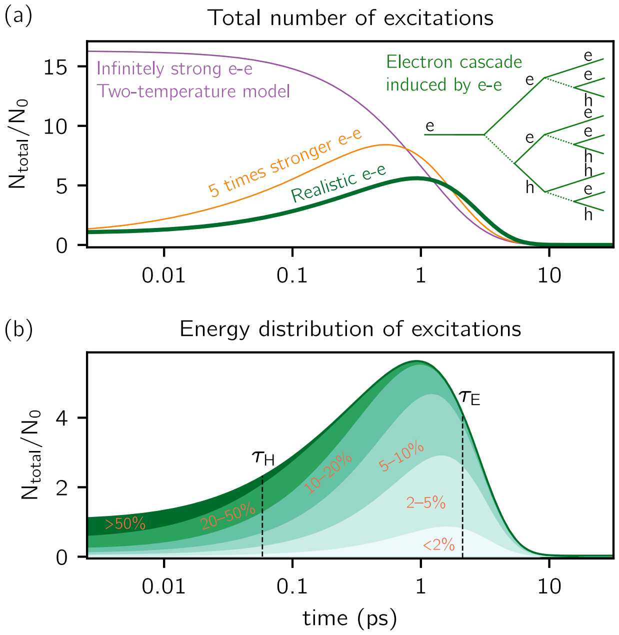

Fig. 2 Dynamics of nonequilibrium electrons after photoexcitation with *hv* = 2 eV. a The total number of nonequilibrium electrons versus time for three different values of electron–electron (e–e) scattering strengths, $\gamma_{ep}/\beta_{ee} \approx 0.25$ (realistic e–e), 0.05 (strong e–e), and 0 (infinite e–e). For the case of infinitely strong electron–electron scattering, the initial distribution evolves instantaneously into a thermal distribution, which increases the number of hot electrons by a factor of ~16. The inset illustrates the cascade dynamics of nonequilibrium electrons, e, and nonequilibrium holes, h. **b** The energy distribution of excitations for the case of $\gamma_{ep}/\beta_{ee} \approx 0.25$. Each band represents the number of excitations in a specific energy range, e.g., the number of excitations with energy greater than 50% of *hv* for the top most dark green band. τ_H is the time-scale that high energy electronic states remain occupied. τ_E is the time-scale for energy transfer between the electronic subsystem and lattice.

assumptions. In general, C will depend on $\phi(\varepsilon, t = 0)$ and the energy dependence of the e–e scattering times. τ_H depends solely on the e–e interaction strength for two reasons.

First, e–e scattering causes much larger changes in the average energy per excitation than e–p interactions. For an electron at energy $\varepsilon = h\nu$, the most probable amount of energy exchanged in an e–e interaction is $h\nu$[25]. Alternatively, an e–p interaction will, on average, change the electron's energy by $\hbar\langle\omega\rangle$. Here, $\hbar\langle\omega\rangle$ is the average phonon energy of the metal and is typically 50–100× smaller than the photon energy $h\nu$. The second reason e–e interactions dominate τ_H is related to the number of in vs. out scattering events for high energy excitations. Nearly all e–e scattering events relax high energy excitations, but only a fraction of e–p scattering events do the same. There are three types of e–p interactions in the e–p collision integral: spontaneous phonon emission, stimulated phonon emission, and phonon absorption. Phonon absorption and stimulated emission rates are nearly equal. Phonon absorption increases an electron's energy, while stimulated phonon emission decreases it. As a result, the most important e–p interaction for $\phi(\varepsilon, t)$ is spontaneous phonon emission. The net effect of all e–p interactions on dynamics is a decrease in energy per electron at a rate of $\pi^2 k_B T \gamma_{ep}/3$. If all e–p interactions reduced electron energies, the energy per electron would decrease at a faster rate of $\hbar\langle\omega\rangle\tau_{ep}^{-1}$.

While e–p interactions won't influence τ_H in metals, they will affect the momentum distribution of nonequilibrium electrons. For some phenomena, e.g., energy transport or photocatalysis, the momentum distribution of nonequilibrium electrons is also important.

The relationship we observe in Fig. 3b of $\tau_H \approx C\beta_{ee}^{-1}$ breaks down in the limit of very strong e–p interactions, e.g., $\gamma_{ep}/\beta_{ee} >> 1$, and/or for photon energies less than 1 eV. (Supplementary Note 3 provides a phenomonlogical expression for τ_H that works across a wider range of γ_{ep}/β_{ee} values.) The reason the relationship breaks down for low energy excitation, e.g. $h\nu < 1$ eV, is that a significant percentage of initially excited carriers are within a few hundred meV of the Fermi-level. E–p interactions dominate dynamics near the Fermi-level. In the limit $h\nu > 1$ eV and $\gamma_{ep}/\beta_{ee} >> 1$, the product of τ_H and β_{ee} is not constant,

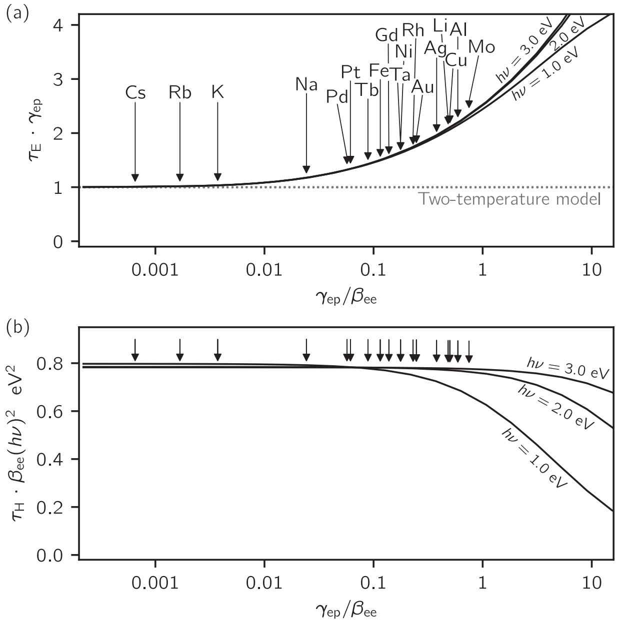

Fig. 3 Dependence of τ_H and τ_E on electron-electron and electron-phonon interaction strengths, β_{ee} and γ_{ep}. To illustrate the universal dependence of τ_E and τ_H on the ratio of interaction strengths γ_{ep}/β_{ee}, we report τ_E and τ_H normalized by the time-scales γ_{ep}^{-1} and β_{ee}^{-1}, respectively. τ_H is the time-scale that high energy electronic states remain occupied. τ_E is the time-scale for energy transfer between the electronic subsystem and lattice. *hv* is the energy of absorbed photons. Values of γ_{ep}/β_{ee} for various metals are indicated with vertical arrows. **a** For realistic values of e–e vs. e–p interaction strengths, τ_E depends on both γ_{ep} and β_{ee}. In the limit of $\gamma_{ep}/\beta_{ee} < 0.05$, τ_E converges to the two-temperature value and is independent of β_{ee}. **b** For photoexcitation with visible light (2 and 3 eV) and realistic values of e–e versus e–p interaction strengths, τ_H depends only on e–e interaction strengths.

meaning τ_H depends on both e–e and e–p interaction strength. However, for metals where literature data is available for both γ_{ep} and β_{ee}, we could find no examples where $\gamma_{ep}/\beta_{ee} >> 1$. Metallic compounds with exceptionally strong e–p interactions, such as Be, VN and MgB$_2$ with $\lambda\langle\omega^2\rangle \approx 2000\,\text{meV}^2$, do not have data available for e–e lifetimes. If these metals possessed weak e–e interaction strengths, e.g., $\beta_{ee}^{-1} > 50$ fs, then τ_H would be sensitive to the e–p interaction strength.

In contrast to τ_H, τ_E is sensitive to both e–e and e–p scattering so long as $\gamma_{ep}/\beta_{ee} > 0.05$. While it is obvious the time-scale for energy transfer from electrons to phonons should depend on e–p scattering strength, the importance of e–e scattering is less straightforward. Unlike e–p scattering, e–e interactions do not change the total energy in the electronic subsystem. Instead, e–e interactions alter how energy is distribtued across the electronic subsystem. Electron–electron scattering events turn a single excited electron into three excited electrons. Three electrons will transfer energy to the phonons roughly three times as fast as one electron because they will spontaneously emit phonons three times as often. As a result, both e–e and e–p interactions determine τ_E if electronic interactions don't rapidly thermalize the electronic subsystem. The importance of cascade dynamics on energy-transfer rates was originally reported by Tas and Maris[5], as well as others later[23,29,31,39].

The energy relaxation times in Fig. 3 are well approximated as $\tau_E \approx 2.5 \cdot \beta_{ee}^{-0.25}\gamma_{ep}^{-0.75}$ provided $0.05 < \gamma_{ep}/\beta_{ee} < 2$. Alternatively, $\tau_E \approx \gamma_{ep}^{-1} + 1.8\gamma_{ep}^{-1}[1 - \tanh(-0.35\ln[0.6\gamma_{ep}/\beta_{ee}])]$ is a good approximation for all $\gamma_{ep}/\beta_{ee} < 2$. A survey of literature values for e–e and e–p interaction strength suggest most metals fall in the range of $0.05 < \gamma_{ep}/\beta_{ee} < 2$, see Table 1. For these metals, the two-temperature model estimate of τ_E is off by a factor ranging from 1.3 to 3, depending on the ratio γ_{ep}/β_{ee}.

Nonthermal effects are most important in metals with light elements and simple electronic structures where γ_{ep}/β_{ee} is largest, e.g., Al. γ_{ep} is highest in metals with light elements, because small ion mass leads to higher phonon frequencies and stronger electron–phonon coupling. β_{ee} is smallest in metals where phase-space for e–e scattering is limited, e.g., the noble metals. β_{ee} is largest in transition metals where the Fermi-level lies in the d-bands. Partial occupation of d-bands increases the phase-space for e–e scattering processes by allowing interband transitions. All other factors being equal, β_{ee} will be higher in metals with higher charge densities. Screening effects are also important. β_{ee} is smaller in metals where screening is large (higher permittivity in the static limit.) For example, β_{ee} is smaller in Au than Ag due to d-band screening.

In the limit of strong e–e scattering, $\gamma_{ep}/\beta_{ee} < 0.05$, the energy relaxation time converges to the two-temperature model prediction, $\tau_E \approx \gamma_{ep}^{-1}$. In this limit, the relaxation of the nonequilibrium electron distribution occurs in a two-step process. The first step is e–e scattering drives electrons into a distribution that is nearly thermal, i.e., a distribution that maximizes entropy in the electronic subsystem. At this stage, the electrons remain out-of-equilibrium with the phonons, i.e., $T_e \neq T_p$. The second step is the nonequilibrium electrons transfer energy to the lattice on a γ_{ep}^{-1} time-scale. The alkali metals Na, K, Rb, and Cs have sufficiently weak e–p interactions for the two-temperature model to be valid. Pd and Pt are also close to meeting the $\gamma_{ep}/\beta_{ee} < 0.05$ criteria due to strong e–e interactions.

While the two-temperature model will lack predictive power in most systems made up of only one metal, $\gamma_{ep}/\beta_{ee} < 0.05$ is easier to satisfy in bilayer systems composed of different types of metals. In a bilayer, if one metal has strong e–e interactions, while the other has weak e–p interactions, e.g., Pt with Au[14,38], then photoexcited electrons in these systems will relax via a two-step process similar to the one described above for two-temperature behavior[14,16]. First, nonequilibrium electrons will thermalize in the layer with strong e–e scattering. Second, a now thermalized distribution of nonequilibrium electrons will exchange energy with phonons in the metal layer with weak e–p interactions. Several recent experimental studies have observed two-step dynamics in metal bilayer systems[14,16,38].

Now we compare our model predictions for τ_E of Au, Al, and Pt with experiment. While a variety of experimental studies are sensitive to the cooling rates of photoexcited electrons[47], interpretation of such experiments is not straightforward[18,37,53]. Time-resolved measurements of changes in optical properties, e.g., time–domain thermoreflectance or time–domain transient absorption, are common methods for studying nonequilibrium electron dynamics[1,26,33,36,47,54]. Optical properties depend on the excited electron distribution in a complex way and deducing τ_E from decay-rates of thermoreflectance or transient absorption signals is not trivial[18]. Two recent experimental studies on nonequilibrium electron dynamics in Au account for this complexity by modeling of how the nonequilibrium electron distribution correlates to changes in the dielectric function of Au. Both studies conclude nonequilibrium electrons transfer energy to phonons on a 2–3 ps time-scale, in fair agreement with our model's prediction for Au of $\tau_E \approx 2$ ps. Our model predictions for $\tau_E \approx 0.15$ ps in Al and $\tau_E \approx 0.16$ ps in Pt are shorter than experimental values extracted from measurements of nonequilibrium heat transfer in metals. Tas and Maris report $\tau_E \approx 0.23$ ps in Al[5], while Jang et al. report $\tau_E \approx 0.2$ ps for Pt[55].

The reasonable agreement between our prediction of $\tau_{\mathrm{E}} \approx 0.16$ ps for Pt and the Jang et al. experimental value of $\tau_{\mathrm{E}} \approx 0.2$ ps is likely coincidental because there could be error in the value of γ_{ep} we use for Pt. The values of γ_{ep} in Table 1 for all metals were determined in a crude manner based on Debye temperatures and an analysis of experimental electrical resistivity data[56]. Such an approach is likely to have significant error for a metal like Pt, where the electronic density of states is a strong function of energy near the Fermi-level[55].

The discrepancy between the experimental value for Al of $\tau_{\mathrm{E}} \approx 0.23$ ps and our prediction of $\tau_{\mathrm{E}} \approx 0.15$ ps is surprising. Al is often viewed as a nearly free electron metal. Our model assumptions should be most reasonable for free electron like metals. The discrepancy may be due to our estimate of β_{ee}. For Al we set β_{ee}^{-1} to 40 fs for Al based on time-resolved two-photon photoemission data[32]. However, deducing the average e–e scattering rate vs. electron energy from experimental photoemission data is nontrivial. It requires evaluating the effect of a variety of factors on the on the two photon photoemission data. These factors include hot electron transport, surface scattering, e–p interactions, and the wave-vector dependence of e–e scattering rates[32]. For many metals, predictions for β_{ee}^{-1} from the GW approximation[25] agree with photoemission data, e.g., Au (220 vs. 300 fs) and Cu (200 vs. 160 fs). But this is not the case for Al, where GW predicts a electron-momentum averaged value for β_{ee}^{-1} that is ~6× larger than the one deduced from two-photon photoemission measurements[25]. Nechaev et al. have suggested the disagreement is because the two-photon data is a measure of both e–e and e–p interactions in Al[57]. However, Nechaev et al. analysis does not solve an equation of motion for hot electrons like Eq. (1) to include the effect of e–p interactions on the distribution. Instead, Nechaev et al.‘s analysis relies on Matthiesen's rule to add e–e and e–p quasiparticle scattering rates, which is not valid. Schone et al. have suggested that two-photon photoemission experiments are primarily a measure of the lifetime of electrons near the W-point of k-space[58]. Light absorption primarily populates states near the W-point of k-space due to momentum conservation. Near the W-point, the band-structure of Al deviates markedly from a free-electron system[58]. As a result, the e–e quasiparticle lifetime of electronic states near the W-point are much shorter than the average value across the Brillouin zone[58]. Since the time-scale for energy relaxation is much greater than the time-scale for e–e and e–p quasiparticle scattering, τ_{E} will depend on e–e scattering rate of states across the entire Brillouin zone, and not just e–e scattering rates of states near the W-point. If, instead of using two-photon data, we use the electron-momentum averaged GW prediction from Ladstädter et al.[25] to set $\beta_{\mathrm{ee}}^{-1} \approx 260$ fs for Al, our model predicts $\tau_{\mathrm{E}} \approx 0.22$ ps. This latter value is in good agreement with the experimental results of Tas and Maris[5].

While the present study considers the regime of low laser fluence, we expect that at larger fluence the type of dynamics, and relaxation times, will be different. At higher fluence, the dynamics will be closer to the two-step process described by the two-temperature model. This change in dynamics occurs because a higher laser fluence requires fewer e-e scattering events to relax photoexcited electrons to a Fermi–Dirac thermal distribution. To understand why, consider an absorbed fluence of 10 mJ m^{-2} in a 10 nm thick Au film. This energy density spread across a thermal distribution of electrons corresponds to 60 meV per excited electron, much less than eV scale energies of photoexcited electrons. Alternatively, an absorbed fluence of 10 J m^{-2} spread across a thermal distribution of electrons corresponds to ~0.5 eV per excited electron, which is comparable to the energy of photoexcited electrons. Therefore, a distribution excited by a high fluence laser pulse requires fewer e–e scattering events to evolve into a Fermi–Dirac distribution.

Our calculations in Figs. 1–3 were carried out at 300 K, but the results are similar at other temperatures. The rate of energy relaxation will increase at lower temperatures because of decreases in electronic heat capacity, i.e., changes in $f_0(\varepsilon, T)$. Changes to e–p scattering rates due to changes in ambient temperature are relatively unimportant. This is because the rate of energy transfer from nonequilibrium electrons to phonons depends primarily on spontaneous phonon emission, which is temperature independent. The effect of temperature is included in our approximate expression for τ_{E} via the γ_{ep} term.

In conclusion, we have numerically solved the Boltzmann rate equation to quantify how cascade dynamics of photoexcited electrons depend on e–e and e–p interactions. For most simple metals, the rate of energy transfer is sensitive to both e–e scattering and e–p scattering due to cascade dynamics. We find nonthermal effects are most important in metals with light elements and simple electronic structures, e.g., Al and Li. The energy relaxation time of the nonequilibrium electron distribution is well approximated as $\tau_{\mathrm{E}} \approx 2.5 \cdot \beta_{\mathrm{ee}}^{-0.25}\gamma_{\mathrm{ep}}^{-0.75}$, where γ_{ep} is the electron-phonon energy relaxation rate predicted for a thermal electron distribution, and β_{ee} is e–e scattering rate of an electron or hole 0.5 eV away from the Fermi level. In the limit that $\gamma_{\mathrm{ep}}/\beta_{\mathrm{ee}}\,\$\,0.05$, the two-temperature model is accurate because e–e scattering is effective at establishing a near thermal distribution of electrons before significant energy is transferred to the lattice. We can identify only a few metals that satisfy the criterion $\gamma_{\mathrm{ep}}/\beta_{\mathrm{ee}} < 0.05$: Na, K, Rb, and Cs. These findings are important for understanding ultrafast electron dynamics in a diverse range of fields, e.g., ultrafast magnetism, photocatalysis, plasmonics, and others.

Methods

Collision integrals. To solve Eq. (1) we need analytic expressions for the collision integrals. Using a Taylor series expansion, we approximate the electron-phonon collision integral as

$$\Gamma_{\mathrm{ep}}(\phi(\varepsilon, t)) = \pi\hbar\lambda\langle\omega^2\rangle\left[-2\frac{\mathrm{d}f_0(\varepsilon)}{\mathrm{d}\varepsilon}\phi(\varepsilon) + [1 - 2f_0(\varepsilon)]\frac{\partial\phi(\varepsilon)}{\partial\varepsilon} + k_{\mathrm{B}}T\frac{\partial^2\phi(\varepsilon)}{\partial\varepsilon^2}\right]. \tag{3}$$

Here, $\lambda\langle\omega^2\rangle$ is the second frequency moment of the Eliashberg function $\alpha^2F(\omega)\omega^{-1}$,

$$\lambda\langle\omega^2\rangle = 2\int \mathrm{d}\omega\alpha^2F(\omega)\omega. \tag{4}$$

We provide a full derivation of Eq. (3) in Supplementary Note 1. We use the analytic solution for the electron–electron collision integral derived by Kabanov et al.[27] for Fermi liquids

$$\begin{aligned}\frac{\mathrm{d}\phi}{\mathrm{d}t} = &-\frac{\phi(\varepsilon)}{\tau_{\mathrm{ee}}(\varepsilon)} + \frac{K}{\cosh\left(\frac{\varepsilon}{2k_{\mathrm{B}}T}\right)}\int_{-\infty}^{\infty}\mathrm{d}\varepsilon'\phi(\varepsilon')\cosh\left(\frac{\varepsilon'}{2k_{\mathrm{B}}T}\right)\\ &\times\left[\frac{(\varepsilon-\varepsilon')}{\sinh\left(\frac{\varepsilon-\varepsilon'}{2k_{\mathrm{B}}T}\right)} - \frac{(\varepsilon+\varepsilon')}{2\sinh\left(\frac{\varepsilon+\varepsilon'}{2k_{\mathrm{B}}T}\right)}\right]\end{aligned}, \tag{5}$$

where

$$\tau_{\mathrm{ee}}(\varepsilon) = \frac{2}{K}\left(\frac{1}{(\pi k_{\mathrm{B}}T)^2 + \varepsilon^2}\right). \tag{6}$$

Equation (5) redistributes energy in the electronic subsystem while conserving the total energy in the subsystem.

Evaluation of Γ_{ep} in Eq. (3) requires the material's electron–phonon spectral function $\alpha^2F(\varepsilon, \omega)$[23,24,27,29,31] to evaluate the value of $\lambda\langle\omega^2\rangle$ as a function of electron energy ε. Similarly, evaluation of Γ_{ee} in Eq. (5) requires knowledge of the Kernel function $K(\varepsilon, \varepsilon', \varepsilon'', \varepsilon''')$[23,24,27,29,31]. (This function is the Kernel of the e–e collision integral.) The function $\alpha^2F(\varepsilon, \omega)$ is the average square of the electron–phonon matrix element on a constant electron energy surface of ε with phonons of frequency ω. The function $\alpha^2F(\varepsilon, \omega)$ determines average e–p quasiparticle lifetime of electronic states on the constant energy surface ε with a phonon of frequency ω. At the Fermi-level, $\alpha^2F(0, \omega)$ governs many electronic phenomena in metals, e.g., electrical resistivity and superconductivity[59]. The Kernel function $K(\varepsilon, \varepsilon', \varepsilon'', \varepsilon''')$ is the average square of the electron-electron matrix element between electrons on a constant energy surface ε with electronic states on constant energy surfaces defined by ε′, ε″, and ε″ [28]. The Kernel function determines the average e-e quasi-particle lifetime of electronic states on the constant energy surface ε. Like the e–p spectral function, the Kernel function is important for a variety of electronic phenomena in metals. At the Fermi-level, the constant $K(\varepsilon = 0)$ is related to the Coulomb pseudopotential, which is an important for the theory for low-temperature resistivity of transition metals[60] and the theory of superconductivity[27].

To define simple descriptors for the e–e and e–p interaction strengths, we neglect the dependence of $\lambda\langle\omega^2\rangle$ and K on electron energy ε and fix e–e and e–p interaction strengths to their values at the Fermi-level. This assumption is quite good for simple metals like Al, Cu, Ag, Au, as well as the alkali metals. In these metals, the electronic density of states is relatively constant within $h\nu$ of the Fermi-level, which is the energy-scale we are concerned with here. A variety of theoretical and experimental studies provide evidence that neglecting the ε dependence is a reasonable approximation for simple metals. First-principles calculations for Al, Cu, and Au confirm that both $\lambda\langle\omega^2\rangle$[17] and K[25] depend only weakly on ε. An energy independent K leads to the well-known ε^{-2} dependence for electron–hole excitations in a Fermi-liquid, and time-resolved two-photon photoemission measurements of Al, Au, Ag, and Cu observe such an ε^{-2} dependence[32]. Alternatively, in transition metals, the electronic density of states can vary significantly within a few eV of the Fermi level. As a result, our assumption that $\lambda\langle\omega^2\rangle$ and K are independent of ε will cause some error in calculated values of τ_E and τ_H for transition metals. We quantify this error in Supplementary Note 2.

Instead of using $\lambda\langle\omega^2\rangle$ and K as descriptors for the e–e and e–p interaction strengths, we prefer alternative but related parameters that correspond to important time-scales in our problem. As a descriptor of the e–p interaction, we choose the energy-relaxation time for a thermal distribution of nonequilibrium electrons, γ_{ep}. γ_{ep} and $\lambda\langle\omega^2\rangle$ are proportional to one another: $\gamma_{ep} = 3\hbar\lambda\langle\omega^2\rangle/(\pi k_B T)$. The values we used for γ_{ep} of various metals are reported in Table 1. Table 1 values are based on an analysis of electrical resistivity data by Allen[59] and use the approximation $\lambda\langle\omega^2\rangle \approx \lambda \cdot \Theta_D^2/2$, where Θ_D is the Debye temperature. To describe the e–e interaction strength, we choose the scattering rate of a 0.5 eV electronic excitation $\beta_{ee} = K(0.5\,\mathrm{eV})^2/2$. Values for β_{ee} in Table 1 for nonalkali metals are based on photoemission data for electron lifetimes[32]. β_{ee} for the alkali metals is based on predictions of Fermi liquid theory for a homogenous electron gas[32]. We choose the scattering time for 0.5 eV electrons as our measure for e–e interaction strength because this is the lowest energy, where experimental two-photon emission data is commonly available. Alternative descriptor choices for e–e interactions, e.g., the lifetime of 1 eV electrons, would yield quite similar results (see Supplementary Note 2). Fixing the e–e interaction strength with the electron lifetime at 0.5 eV allows Eq. (6) to make reasonably accurate predictions for $\tau_{ee}(\varepsilon < 1\,\mathrm{eV})$ in transistion metals, despite our model neglecting the ε dependence of K, see Supplementary Fig. 4. We want $\tau_{ee}(\varepsilon)$ be accurate for low energy excitations because, as shown in Fig. 2b, nearly all nonequilibrium electrons are at low energies on time-scales comparable to τ_E.

Solving Eq. (1) requires initial conditions. We assume the probability a photon with energy $h\nu$ will move an electron from a state with energy ε to a state with energy $\varepsilon + h\nu$ is proportional to $f_0(\varepsilon)(1 - f_0(\varepsilon + h\nu))$. This assumption results in a flat initial distribution of electrons and holes with concentration $\phi_0 << 1$ that extends to an energy $h\nu$ above and below the Fermi level. We consider $h\nu$ between 1 and 3 eV, i.e., visible light. We focus on visible light because most experimental studies on ultrafast electron dynamics use visible light for photoexcitation. Our conclusions do not rely on the assumption that a flat distribution is excited. We obtain similar results if we assume a completely different energy dependence for the initial distribution. For example, we obtain nearly identical results for how τ_E depends on e–e and e–p scattering strengths if we instead assume photons with energy $h\nu$ only excite electrons and holes at energy $h\nu/2$ above and below the Fermi level.

In our calculations, we assume instantaneous photoexcitation so the relaxation times of $\phi(\varepsilon, t)$ depend only on e–e and e–p interactions. The time-scales τ_E and τ_H describe the intrinsic response times of the metal, and do not depend on pulse duration of the photoexcitation. The effect of a finite pulse duration could be included in several ways. A time-dependent source term could be added to Eq. (1). Or, our solution for $\phi(\varepsilon, t)$ in response to initial conditions could be used to construct a Green's function solution to the problem.

Model assumptions. For completeness, we now summarize all the assumptions in our model. Equation (1) assumes the distribution function depends only on energy and time, thereby neglecting variation in angles of the wavevector. When solving Eq. (1), we neglect any rise in internal energy of the lattice, i.e., we assume T_p is constant. This assumption is reasonable because the phonon heat-capacity is large compared to the electron heat capacity. Furthermore, allowing T_p to evolve with time wouldn't affect predictions for τ_H and τ_E because T_p doesn't affect the two most important types of scattering processes: e–e scattering rates and spontaneous phonon emission rates. For some applications, e.g., photocatalysis, the increase in T_p is important to track so that thermal and nonequilibrium electron phenomena can be differentiated[21,22]. The effects of a dynamic phonon temperature can be added to our model by solving the equation $C_p \frac{\partial T_p}{\partial t} = -\frac{\partial E_{tot}}{\partial t}$ simultaneously with Eq. (1), where E_{tot} is the energy stored by the nonequilibrium electron distribution. Another assumption we make when solving Eq. (1) is low fluence photoexcitation. We linearize Eq. (1) by assuming $\phi(\varepsilon, t) = f(\varepsilon, t) - f_0(\varepsilon) \ll 1$, and keeping only terms linear in $\phi(\varepsilon, t)$. As noted above, we neglect the dependence of the e–p spectral function on electron energy, and the dependence of the e–e Kernel function on electron energy. Finally, by setting the initial distribution to $\phi(\varepsilon, t = 0) = \phi_0$ at all energies within $h\nu$ of the Fermi-level, we are assuming an energy independent joint density of states. These latter three assumptions are all related to the energy dependence of the electronic density of states. We discuss why these latter three assumptions are reasonable in Supplementary Note 2.

Data availability

The datasets generated during and/or analysed during the current study are available from the corresponding author on reasonable request

Received: 22 May 2020; Accepted: 4 September 2020;

References

1. Fann, W., Storz, R., Tom, H. & Bokor, J. Electron thermalization in gold. *Phys. Rev. B* **46**, 13592 (1992).
2. Fann, W., Storz, R., Tom, H. & Bokor, J. Direct measurement of nonequilibrium electron-energy distributions in subpicosecond laser-heated gold films. *Phys. Rev. Lett.* **68**, 2834 (1992).
3. Christopher, P. & Moskovits, M. Hot charge carrier transmission from plasmonic nanostructures. *Annu. Rev. Phys. Chem.* **68**, 379–398 (2017).
4. Ritchie, R. H. Coupled electron-hole cascade in a free electron gas. *JAP* **37**, 2276–2278 (1966).
5. Tas, G. & Maris, H. J. Electron diffusion in metals studied by picosecond ultrasonics. *Phys. Rev. B* **49**, 15046–15054 (1994).
6. Wilson, R. B. et al. Electric current induced ultrafast demagnetization. *Phys. Rev. B* **96**, 045105 (2017).
7. Wilson, R. B. et al. Ultrafast magnetic switching of GdFeCo with electronic heat currents. *Phys. Rev. B* **95**, 180409 (2017).
8. Yang, Y. et al. Ultrafast magnetization reversal by picosecond electrical pulses. *Sci. Adv.* https://doi.org/10.1126/sciadv.1603117 (2017).
9. Battiato, M., Carva, K. & Oppeneer, P. M. Superdiffusive spin transport as a mechanism of ultrafast demagnetization. *Phys. Rev. Lett.* **105**, 027203 (2010).
10. Schellekens, A., Kuiper, K., De Wit, R. & Koopmans, B. Ultrafast spin-transfer torque driven by femtosecond pulsed-laser excitation. *Nat. Commun.* **5**, 4333 (2014).
11. Choi, G.-M., Moon, C.-H., Min, B.-C., Lee, K.-J. & Cahill, D. G. Thermal spin-transfer torque driven by the spin-dependent Seebeck effect in metallic spin-valves. *Nat. Phys.* **11**, 576 (2015).
12. Seifert, T. S. et al. Femtosecond formation dynamics of the spin Seebeck effect revealed by terahertz spectroscopy. *Nat. Commun.* **9**, 2899 (2018).
13. Alekhin, A. et al. Femtosecond spin current pulses generated by the nonthermal spin-dependent seebeck effect and interacting with ferromagnets in spin valves. *Phys. Rev. Lett.* **119**, 017202 (2017).
14. Choi, G.-M., Wilson, R. & Cahill, D. G. Indirect heating of Pt by short-pulse laser irradiation of Au in a nanoscale Pt/Au bilayer. *Phys. Rev. B* **89**, 064307 (2014).
15. Battiato, M., Carva, K. & Oppeneer, P. M. Theory of laser-induced ultrafast superdiffusive spin transport in layered heterostructures. *Phys. Rev. B* **86**, 024404 (2012).
16. Pudell, J. et al. Layer specific observation of slow thermal equilibration in ultrathin metallic nanostructures by femtosecond X-ray diffraction. *Nat. Commun.* **9**, 3335 (2018).
17. Brown, A. M., Sundararaman, R., Narang, P., Goddard, W. A. & Atwater, H. A. Ab initio phonon coupling and optical response of hot electrons in plasmonic metals. *Phys. Rev. B* **94**, 075120 (2016).
18. Brown, A. M. et al. Experimental and ab initio ultrafast carrier dynamics in plasmonic nanoparticles. *Phys. Rev. Lett.* **118**, 087401 (2017).
19. Kale, M. J. & Christopher, P. Plasmons at the interface. *Science* **349**, 587–588 (2015).
20. Linic, S., Aslam, U., Boerigter, C. & Morabito, M. Photochemical transformations on plasmonic metal nanoparticles. *Nat. Mater.* **14**, 567 (2015).
21. Dubi, Y. & Sivan, Y. "Hot" electrons in metallic nanostructures—non-thermal carriers or heating? *Light Sci. Appl.* **8**, 89 (2019).
22. Sivan, Y., Un, I. W. & Dubi, Y. Assistance of metal nanoparticles in photocatalysis—nothing more than a classical heat source. *Faraday Discuss.* **214**, 215–233 (2019).
23. Rethfeld, B., Kaiser, A., Vicanek, M. & Simon, G. Ultrafast dynamics of nonequilibrium electrons in metals under femtosecond laser irradiation. *Phys. Rev. B* **65**, 214303 (2002).
24. Mueller, B. & Rethfeld, B. Relaxation dynamics in laser-excited metals under nonequilibrium conditions. *Phys. Rev. B* **87**, 035139 (2013).

25. Ladstädter, F., Hohenester, U., Puschnig, P. & Ambrosch-Draxl, C. First-principles calculation of hot-electron scattering in metals. *Phys. Rev. B* **70**, 235125 (2004).
26. Lin, Z., Zhigilei, L. V. & Celli, V. Electron-phonon coupling and electron heat capacity of metals under conditions of strong electron-phonon nonequilibrium. *Phys. Rev. B* **77**, 075133 (2008).
27. Kabanov, V. V. & Alexandrov, A. Electron relaxation in metals: theory and exact analytical solutions. *Phys. Rev. B* **78**, 174514 (2008).
28. Allen, P. B. Theory of thermal relaxation of electrons in metals. *Phys. Rev. Lett.* **59**, 1460–1463 (1987).
29. Groeneveld, R. H. M., Sprik, R. & Lagendijk, A. Femtosecond spectroscopy of electron-electron and electron-phonon energy relaxation in Ag and Au. *Phys. Rev. B* **51**, 11433–11445 (1995).
30. Del Fatti, N., Bouffanais, R., Vallée, F. & Flytzanis, C. Nonequilibrium electron interactions in metal films. *Phys. Rev. Lett.* **81**, 922–925 (1998).
31. Del Fatti, N. et al. Nonequilibrium electron dynamics in noble metals. *Phys. Rev. B* **61**, 16956–16966 (2000).
32. Bauer, M., Marienfeld, A. & Aeschlimann, M. Hot electron lifetimes in metals probed by time-resolved two-photon photoemission. *Prog. Surf. Sci.* **90**, 319–376 (2015).
33. Hopkins, P. E., Kassebaum, J. L. & Norris, P. M. Effects of electron scattering at metal-nonmetal interfaces on electron-phonon equilibration in gold films. *JAP* **105**, 023710 (2009).
34. Chase, T. et al. Ultrafast electron diffraction from non-equilibrium phonons in femtosecond laser heated Au films. *APL* **108**, 041909 (2016).
35. Della Valle, G., Conforti, M., Longhi, S., Cerullo, G. & Brida, D. Real-time optical mapping of the dynamics of nonthermal electrons in thin gold films. *Phys. Rev. B* **86**, 155139 (2012).
36. Hohlfeld, J. et al. Electron and lattice dynamics following optical excitation of metals. *Chem. Phys.* **251**, 237–258 (2000).
37. Waldecker, L., Bertoni, R., Ernstorfer, R. & Vorberger, J. Electron-phonon coupling and energy flow in a simple metal beyond the two-temperature approximation. *Phys. Rev. X* **6**, 021003 (2016).
38. Wang, W. & Cahill, D. G. Limits to thermal transport in nanoscale metal bilayers due to weak electron-phonon coupling in Au and Cu. *Phys. Rev. Lett.* **109**, 175503 (2012).
39. Gusev, V. E. & Wright, O. B. Ultrafast nonequilibrium dynamics of electrons in metals. *Phys. Rev. B* **57**, 2878–2888 (1998).
40. Pietanza, L., Colonna, G., Longo, S. & Capitelli, M. Non-equilibrium electron and phonon dynamics in metals under femtosecond laser pulses. *Eur. Phys. J. D* **45**, 369–389 (2007).
41. Brown, A. M., Sundararaman, R., Narang, P., Goddard, W. A. III & Atwater, H. A. Nonradiative plasmon decay and hot carrier dynamics: effects of phonons, surfaces, and geometry. *Acs Nano* **10**, 957–966 (2015).
42. Shin, H.-H., Koo, J.-J., Lee, K. S. & Kim, Z. H. Chemical reactions driven by plasmon-induced hot carriers. *Appl. Mater. Today* **16**, 112–119 (2019).
43. Cortés, E. et al. Plasmonic hot electron transport drives nano-localized chemistry. *Nat. Commun.* **8**, 14880 (2017).
44. Avanesian, T. & Christopher, P. Adsorbate specificity in hot electron driven photochemistry on catalytic metal surfaces. *J. Phys. Chem. C* **118**, 28017–28031 (2014).
45. Saavedra, J., Asenjo-Garcia, A. & García de Abajo, F. J. Hot-electron dynamics and thermalization in small metallic nanoparticles. *ACS Photonics* **3**, 1637–1646 (2016).
46. Khurgin, J. B. Fundamental limits of hot carrier injection from metal in nanoplasmonics. *Nanophotonics* **9**, 453–471 (2020).
47. Brorson, S. et al. Femtosecond room-temperature measurement of the electron-phonon coupling constant γ in metallic superconductors. *Phys. Rev. Lett.* **64**, 2172 (1990).
48. Bernardi, M., Mustafa, J., Neaton, J. B. & Louie, S. G. Theory and computation of hot carriers generated by surface plasmon polaritons in noble metals. *Nat. Commun*. **6**, 1–9 (2015).
49. Bernardi, M., Vigil-Fowler, D., Lischner, J., Neaton, J. B. & Louie, S. G. Ab initio study of hot carriers in the first picosecond after sunlight absorption in silicon. *Phys. Rev. Lett.* **112**, 257402 (2014).
50. Carpene, E. Ultrafast laser irradiation of metals: beyond the two-temperature model. *Phys. Rev. B* **74**, 024301 (2006).
51. Wilson, R. B., Feser, J. P., Hohensee, G. T. & Cahill, D. G. Two-channel model for nonequilibrium thermal transport in pump-probe experiments. *Phys. Rev. B* **88**, 144305 (2013).
52. Carpene, E. et al. Dynamics of electron-magnon interaction and ultrafast demagnetization in thin iron films. *Phys. Rev. B* **78**, 174422 (2008).
53. Heilpern, T. et al. Determination of hot carrier energy distributions from inversion of ultrafast pump-probe reflectivity measurements. *Nat. Commun.* **9**, 1853 (2018).
54. Wellstood, F. C., Urbina, C. & Clarke, J. Hot-electron effects in metals. *Phys. Rev. B* **49**, 5942–5955 (1994).
55. Jang, H., Kimling, J. & Cahill, D. G. Nonequilibrium heat transport in Pt and Ru probed by an ultrathin Co thermometer. *Phys. Rev. B* **101**, 064304 (2020).
56. Allen, P. B. Empirical electron-phonon values from resistivity of cubic metallic elements. *Phys. Rev. B* **36**, 2920–2923 (1987).
57. Nechaev, I., Sklyadneva, I. Y., Silkin, V. M., Echenique, P. M. & Chulkov, E. V. Theoretical study of quasiparticle inelastic lifetimes as applied to aluminum. *Phys. Rev. B* **78**, 085113 (2008).
58. Schöne, W.-D., Keyling, R., Bandić, M. & Ekardt, W. Calculated lifetimes of hot electrons in aluminum and copper using a plane-wave basis set. *Phys. Rev. B* **60**, 8616 (1999).
59. Allen, P. B. Empirical electron-phonon λ values from resistivity of cubic metallic elements. *Phys. Rev. B* **36**, 2920 (1987).
60. Volkenshtein, N., Dyakina, V. & Startsev, V. Scattering mechanisms of conduction electrons in transition metals at low temperatures. *Phys. Status Solidi* **57**, 9–42 (1973).
61. Kittel, C., McEuen, P. & McEuen, P. *Introduction to Solid State Physics*. 8 (Wiley, New York, 1996).
62. Papaconstantopoulos, D. et al. Calculations of the superconducting properties of 32 metals with Z ≤ 49. *Phys. Rev. B* **15**, 4221 (1977).

Acknowledgements

The work by R. Wilson was supported by the U.S. Army Research Laboratory and the U.S. Army Research Office under contract/grant number W911NF-18-1-0364. The work by S. Coh was supported by NSF DMR-1848074.

Author contributions

R.B.W. developed the model. R.B.W. and S.C. designed the study, performed calculations, and wrote the manuscript.

Competing interests

The authors declare no competing interests.

Additional information

Supplementary information is available for this paper at https://doi.org/10.1038/s42005-020-00442-x.

Correspondence and requests for materials should be addressed to R.B.W. or S.C.

Reprints and permission information is available at http://www.nature.com/reprints